University of Huddersfield Repository

To, Suet, Zhu, Zhiwei and Zeng, Wenhan

Novel end-fly-cutting-servo system for deterministic generation of hierarchical micro–nanostructures

Original Citation

This version is available at http://eprints.hud.ac.uk/id/eprint/27317/

http://eprints.hud.ac.uk/

Novel end-fly-cutting-servo system for deterministic generation of hierarchical micro–nanostructures

Suet To (3)[a,b,*], Zhiwei Zhu[a], Wenhan Zeng[c]

[a]State Key Laboratory of Ultra-precision Machining Technology, Department of Industrial and Systems Engineering, The Hong Kong Polytechnic University, Kowloon, Hong Kong Special Administrative Region
[b]Shenzhen Research Institute of the Hong Kong Polytechnic University, Shenzhen, PR China
[c]University of Huddersfield, UK
Submitted by Xiangqian Jiang, University of Huddersfield, UK

Abstract: This paper reports on the diamond cutting based generation of hierarchical micro–nanostructures, which are conventionally difficult for both mechanical and non-mechanical methods to achieve. A novel end-fly-cutting- servo (EFCS) system, with four-axis servo motions that combine the concepts of fast/slow tool servo and endface fly-cutting, is proposed and investigated. In the EFCS system, an intricately shaped primary surface is generated by material removal, while the desired secondary nanostructures are simultaneously constructed using residual tool marks by actively controlling tool loci. The potential of the EFCS system is demonstrated firstly by fabricating a nanostructured F-theta freeform surface and a nanostructured micro-aspheric array.

Keywords: Ultra precision Cutting Micromachining Nanostructure

1. Introduction

Mimicking bio-surface featuring hierarchical micro–nano architecture leads to inconceivable impacts on optical, mechanical, frictional, biological, and interfacial properties of artificial components [1] and [2]. Currently, a variety of machining methods have been established for generating the multi-scale surfaces, including soft lithography, self-assembly, soft nano-imprinting, laser based two photon polymerization, reactive-ion and laser etching, chemical synthesis and electrochemical processing [2], [3] and [4]. However, these methods are commonly restricted with respect to specified material, long processing time, complex operations and expensive costs. Besides, it is still a crucial task for a major of them to flexibly generate hierarchical micro–nanostructures with an accurate primary complicated surface and an ordered secondary nanostructure [3] and [4].

Mechanical machining, especially diamond cutting, is widely regarded as more universal and deterministic due to the capacity of generating intricate surfaces with submicron form accuracy and nanometric surface roughness on a wide spectrum of engineering materials. By means of fast tool servo (FTS) or slow tool servo (STS), hierarchical macro–microstructures can be well obtained; for example, the true three dimensional (3D) artificial compound eyes [5] and [6]. The scale of obtained secondary structures is often limited to an order of several hundred micrometres, and it is also hard to generate discontinuous structures with very sharp edges due to its limited dynamic response. Although the recently developed nano-FTS could fabricate very complicated nano-structures, the nano-level stroke and finite bandwidth restrict its applications in obtaining large-area hierarchical structures [7]. Another diamond cutting method, namely the fly-cutting, is very promising for the generation of sharp-edged structures [8]. However, it is often of extremely low efficiency and is limited to flat primary surfaces.

To obtain much smaller scales of secondary structures, ultrasonic elliptical vibration texturing (UEVT) method was proposed to generate micro-dimple patterns and textured micro-channels [9] and [10]. Another rotary ultrasonic texturing (RUT) method, combining rotation and ultrasonic vibration of a one-point diamond tool, was developed to obtain micro-grooves with imposition of wavy nanostructures [11]. Both UEVT and RUT are promising for surface patterning due to the high efficiency and low dimensional scale, with both being induced by ultrasonic vibrations. However, they are sufficient for flat surfaces but are difficult for processing intricately shaped primary surfaces.

As discussed above, it is still a challenge for both mechanical and non-mechanical processes to flexibly generate hierarchical micro–nanostructures. In this study, a novel end-fly-cutting-servo (EFCS) system combining the concepts of FTS/STS and fly-cutting is proposed for the generation of the multi-scale structures.

2. End-fly-cutting-servo system

The concepts of FTS/STS and end-face fly-cutting are synthesized to complement each other, resulting in the novel EFCS system with enhanced machining capacity. In the following, details of its basic principle, system configuration, and surface generation mechanism are presented.

2.1. Basic principle of the EFCS system

In diamond cutting, relative motion between the diamond tool and the workpiece finally determines the shape of machined surface. On this basis, the required motion for generating the unique structures is identified and reallocated to the four-axis servo motions of the ultra-precision machine tool.

To generate sharp-edged structures, intersection of the tool loci over the workpiece is adopted. In FTS/STS turning, it is operated in the cylindrical coordinate system, where the cutting direction is always perpendicular to the polar axis of the workpiece. Thus, it is impossible to construct the intersections. With the EFCS system, the diamond tool is installed on the spindle and rotated with it; meanwhile, the workpiece is clamped on the slide. Essentially, the cutting operation is transferred to the Cartesian coordinate system. Thus, a variety of relative cutting directions can be obtained with respect to the workpiece due to the circular motion of the diamond tool.

Translational servo motions along the Z-axis of the machine tool were inherited from FTS/STS and rearranged at the workpiece to be responsible for deterministic generation of the intricately shaped primary surfaces. Simultaneously, side feeding along the direction approximately perpendicular to the cutting direction is adopted to make the material removal cover the whole workpiece. Overall, two different kinds of surface generation mechanisms are adopted in the EFCS system: the primary desired surface (PDS) is formed by material removal, just as in conventional cutting; while the secondary nanostructures are constructed by means of actively controlling the residual tool marks (RTM).

2.2. Configuration of the EFCS system

Fig. 1(a) illustrates the configuration of the EFCS system, which consists of four-axis servo motions, namely X-, Y-, Z- and C-axis. The diamond tool is installed on the fixture and then attached on the spindle. The workpiece is clamped on the slide and follows the translational servo motions along the Z-axis to generate the intricately shaped PDS. Taking advantage of the X- and Y-axis, relative positions between the spindle axis oszsand the workpiece can be adjusted, resulting in a variety of relative cutting directions as shown in Fig. 1(b). By combining these directions, a variety of intersection modes of the cutting loci can be obtained, accordingly

generating arbitrary polyhedron nanostructures on the well-defined PDS. As discussed above, side feeding along the directions shown inFig. 1(b) should be adopted to cover the whole surface, which also requires cooperation of the two servo motions along the X- and Y-axis. Considering the rotations of the diamond tool (C-axis), the EFCS system is essentially a four-axis motion assisted diamond cutting.
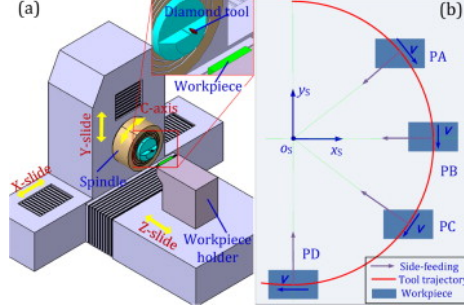

Fig. 1. Configuration of (a) the EFCS system and (b) the induced cutting modes, where os–xsys denotes the coordinate system fixed on the spindle axis, and v denotes the relative cutting speed

2.3. Secondary nanostructure generation in the EFCS system

Since the generation of the PDS in the EFCS system follows the principle of FTS/STS, only the mechanism for the secondary nanostructures, especially the typical nano-pyramids, is detailed here. To fabricate the nano-pyramids, two cutting directions at the positions PB and PD as shown in Fig. 1(b) are employed, which corresponds to the vertical and horizontal cutting modes (VCM & HCM), respectively. Further illustration of the two modes is presented in Fig. 2. If the distance between the spindle axis and theOw–XwZw plane is kept as h/2 during cutting, it forms the VCM. If the distance between the spindle axis and the Ow–YwZw plane is kept as w/2, it forms the HCM. With the VCM, the PDS with approximately linear RTMs along the vertical direction could be obtained. By conducting sequential cutting in the HCM, approximately orthogonal intersections of the tool loci in the two modes could result in the nano-pyramids on the PDS as illustrated in Fig. 2(b).
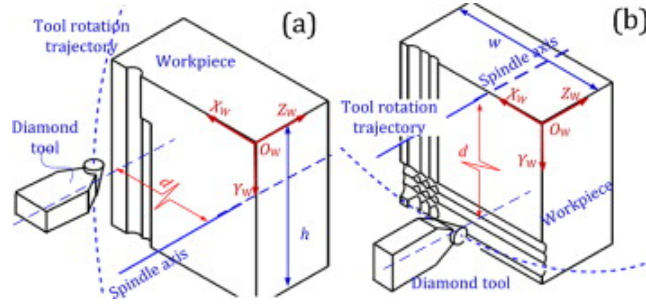

Fig. 2. Schematic of (a) the VCM and (b) the HCM, where O_w-$X_wY_wZ_w$ is the coordinate system on the workpiece; d denotes the rotation radius of the diamond tool; h and w are dimensional parameters of the workpiece.

Assuming that the rotation radius of the tool is larger than the width of the cutting area, the projected tool loci along one cutting direction could be regarded as parallel arcs. Thus, with respect to the round edge of the diamond tool, analytical height and width of the RTMs at any given point can be estimated by [12]

$$h_p = \begin{cases} R_t - \sqrt{R_t^2 - 0.25f^2}, \text{if } \rho = \infty; \\ \dfrac{\rho}{|\rho|}\sqrt{(\rho + R_t)^2 - 0.25f^2} - \sqrt{R_t^2 - 0.25f^2} - \rho, \text{otherwise.} \end{cases} \quad (1)$$

$$d_{p} = \sqrt{\frac{8h_{p}R_{t}\rho}{R_{t} + \rho}} \qquad (2)$$

where Rt is the nose radius of the tool, f denotes the side feedrate per revolution, and ρ denotes the reciprocal of the local curvature of the PDS in the side-feeding direction.

As shown in Eq. (1) and Eq. (2), the height and width of the pyramid structures are highly dependent on tool geometries, side feedrates, and local curvatures of the PDS. By deliberately choosing the cutting parameters, sizes of the secondary nano-structures can be actively controlled to meet the design requirements.
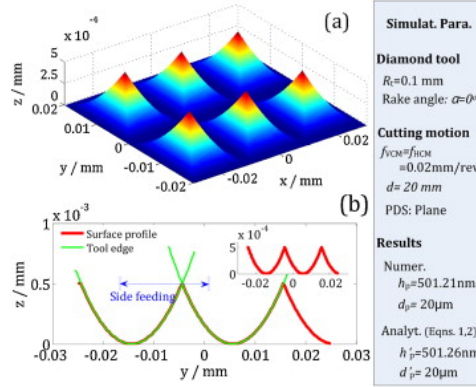

Fig. 3. Structure characteristics obtained by numerical simulation, (a) the 3D structure and (b) the 2D profile.

Taking the nano-pyramids on the planar surface, a numerical simulation was conducted under the specified conditions presented in Fig. 3 to characterize the secondary nano-structures as well as its generation mechanism. The obtained theoretical 3D nano-pyramids and the cross-sectional profile passing the apexes are shown in Fig. 3(a) and Fig. 3(b), respectively. As shown in Fig. 3(b), the profile features sharp nodes and round connections, which may correspond to the intersection and the edge profile of the diamond tool, respectively. The theoretical heights and widths of the nano-pyramids obtained by numerical simulation and analytical calculation agree well with each other as shown in Figure 3. Following the governing law shown in Eq. (1) and Eq. (2), proper parameters for a given structure could be determined.

3. Experimental results and discussion

Cutting experiments were performed on a commercial CNC ultra-precision lathe (Moore Nanotech 350FG, USA) with four-axis servo motions. A homemade fixture with mass balancing was designed to hold the diamond tool. A natural single crystal diamond with round edge, which had nose radius of 0.104 mm and rake angle of 0°, was employed in the cutting. After cutting, the Optical Surface Profiler (Zygo Nexview) was employed to capture topographies of the machined surfaces with effective magnifications.

3.1. Generation of the hierarchical micro–nanostructures

A typical F-theta freeform surface was employed as the PDS. The nano-pyramids were generated on the whole surface to demonstrate the effectiveness of the EFCS system. Both the feedrates along the X- and Y-axis in VCM and HCM were set as fVCM = fHCM = 20 μm/rev.

Fig. 4(a) illustrates the original topography of the obtained hierarchical surface captured with an amplification of 5×, where the lateral resolution is 0.824 μm. To characterize this structure, a two stage process was adopted, including the filter based structure separation and the registration

based form evaluation. To attenuate the edge distortions in conventional Gaussian based filtering, an improved second-order robust Gaussian regression filter was firstly employed to separate the PDS and the nano-pyramids [13], and then the registration method based on the well-known iterative closest point (ICP) algorithm was used for the registration [14]. Accordingly, the filtered one of the surface shown in Fig. 4(a) and the registered PDS are illustrated in Fig. 4(b). A good agreement between the two surfaces was obtained, showing a high machining accuracy of the EFCS system.
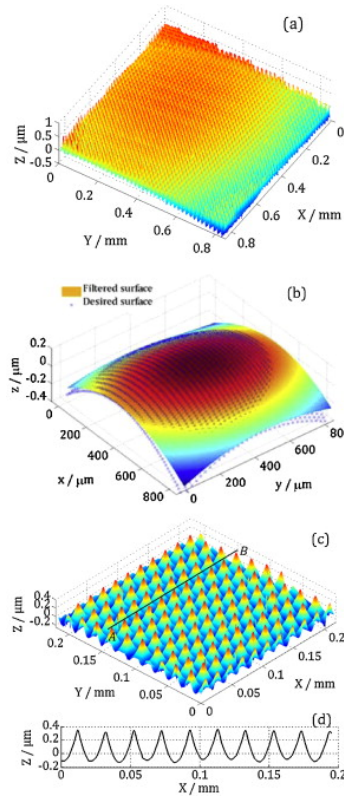

Fig. 4. Characterizations of (a) the freeform surface with nano-pyramids; (b) the filtered primary surface and its registration; and (c) the nano-pyramids on the primary surface.

To allow a more detailed investigation of the secondary nano-pyramids, an amplification of 20× with lateral resolution of 0.211 µm was employed to capture an enlarged view of a partial zone of the surface which is shown in Fig. 4(c) with the primary curvature removed. It is shown that homogenously structured nano-pyramids are obtained that possess similar features to the theoretical ones shown in Fig. 3. A 2D profile in the AB cross-section was extracted as shown in Fig. 4(d), from which uniform structures of the nano-pyramids were obtained with a mean height of 439 nm and a standard deviation of 21 nm. The mean and standard deviation value of the pitch was 20.2 µm and 0.3 µm, respectively.

Another type of ellipsoid micro-aspheric array (MAA) with nano-pyramids was also fabricated. The aperture of each micro-aspheric structure was 200 µm, and the distance between any two successive micro-aspheric structures was 250 µm. Both the feedrates along the *X*- and *Y*-axis in VCM and HCM were also set as fVCM = fHCM = 20 µm/rev.

Characteristics of the obtained structures are shown in Fig. 5. By means of stitching, a large area containing 18 micro-aspheric structures with secondary nano-pyramids was captured with an amplification of 5× and is illustrated in Fig. 5(a). An enlarged view of an arbitrary micro-aspheric structure was also captured with an amplification of 20× as shown in Fig. 5(b). Since each one was rotationally symmetrical, a 2D profile passing the centre, namely in the *AB* cross-section, was

extracted to investigate the machining accuracy, resulting in the profiles shown in Fig. 5(c). A good agreement between the practical and the desired primary profiles was also observed. The mean and standard deviation of the height was 395 nm and 15 nm, respectively. Besides, the mean and standard deviation of the pitch was 18.7 μm and 0.4 μm, respectively. Similarly, the secondary nano-pyramids were further extracted as shown in Fig. 5(d) where homogenous nano-pyramids were achieved, resulting in the nanostructured MAA.
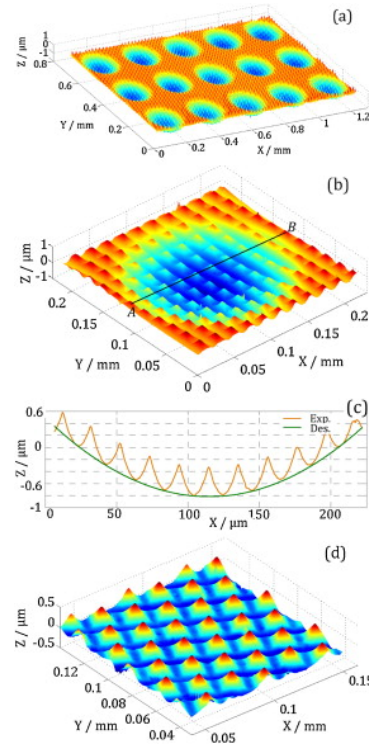

Fig. 5. Characterizations of (a) the MAA with nano-pyramids; (b) a single micro-aspheric structure with nano-pyramids; and (c) the enlarged view of the secondary nano-pyramids.

With the nano-pyramids, the designed heights for the two surfaces were 482 nm and 445 nm, and the designed pitches were 20 μm and 18.5 μm. Comparing with the practical results, there was a good agreement. However, a slight deviation below 10% was observed, which might be jointly caused by material deformation, error motion and measurement error.

3.2. Uniqueness of the EFCS system

In the EFCS system, RTMs are adopted to form the secondary nano-pyramids by actively controlling intersections of the tool loci. Compared with FTS/STS, this makes the generation of nanostructures free from dependence on mechatronic system dynamics. Instead, the dependences are shifted to the geometries and feedrates of the diamond tool, which are much easier to satisfy in cutting. Thus, the shift provides a beneficial basis for the generation of secondary structures with much smaller size scales.

There are also various cutting directions that can be chosen to construct intersections in fly-cutting. By adopting the structure generation mechanism in the EFCS system, it is also possible to fabricate hierarchical structures. However, the efficiency of fly-cutting is extremely low. Due to the lack of translational servo motion and the large swing distance of the diamond tool, it is also hard to generate the micro-structured primary surface, or even freeform surfaces with large curvature variations. In the EFCS system, the point removal mode in fly-cutting is replaced by line removal to significantly improve the efficiency of the EFCS system. Taking advantage of the

ultra-fine servo motions inherited from FTS/STS, an intricately shaped primary surface can be obtained.

There are also some universal advantages for machining that are derived from the unique cutting principle of the EFCS system, such as:

- Operating in the Cartesian coordinate system makes the EFCS system beyond the limitation of position-dependent cutting velocity in FTS/STS, accordingly breaking down the uneven requirements of tracking bandwidth in cutting complicated PDSs, especially the micro-structured surfaces.
- The commonly adopted sampling of the azimuth with even angle intervals leads to uniform quality of the workpiece in the cutting zone, making the EFCS system free from the inconsistent effects of sampling in FTS/STS.
- The EFCS system only adopts part of the cutting cycle, resulting in the interrupted nature of the process. This enables sufficient cooling of the diamond tool in cutting, which might be beneficial for extending tool life [15] and [16].

These unique advantages make the EFCS system not only suitable for hierarchical micro–nanostructures, but also suitable for conventional freeform surface generation. By adopting raster motions, the EFCS system is also promising for large-area fabrication of hierarchical micro–nanostructures with high efficiency.

4. Summary

As a new mechanical machining process for the generation of hierarchical micro–nanostructures, this paper proposes a novel end-fly-cutting-servo (EFCS) system. A variety of properties derived from the unique cutting principles of the EFCS system provide a solid basis for the generation of micro–nanostructures, without restriction of the machine tool dynamics. By combining different cutting directions in the EFCS system, a variety of nano-polygons can be generated as the secondary structure. Herein, the nano-pyramids, which are popular in advanced optical applications, are experimentally generated on a F-theta freeform surface and a micro-aspheric array with high accuracy. It demonstrates that the EFCS is very promising for generating nanostructured freeform surfaces, especially hybrid hierarchical micro–nanostructures.

Acknowledgments

References

[1] Malshe, K. Rajurkar, A. Samant, H.N. Hansen, S. Bapat, W. Jiang, Bio-inspired Functional Surfaces for Advanced Applications, CIRP Annals – Manufacturing Technology, 62 (2) (2013), pp. 607–628

[2] K.-H. Jeong, J. Kim, L.P. Lee,Biologically Inspired Artificial Compound Eyes, Science, 312 (5773) (2006), pp. 557–561

[3] J. Shao, Y. Ding, W. Wang, X. Mei, H. Zhai, H. Tian, X. Li, B. Liu, Generation of Fully Covering Hierarchical Micro-/Nanostructures by Nanoimprinting and Modified Laser Swelling, Small, 10 (13) (2014), pp. 2595–2601

[4] J. Feng, M.T. Tuominen, J.P. Rothstein, Hierarchical Superhydrophobic Surfaces Fabricated by Dual-Scale Electron-Beam-Lithography With Well-Ordered Secondary Nanostructures, Advanced Functional Materials, 21 (2011), pp. 3715–3722

[5] L. Li, A.Y. Yi, Development of a 3D Artificial Compound Eye, Optics Express, 18 (2010), pp. 18125–18137

[6] S. Scheiding, A.Y. Yi, A. Gebhardt, L. Li, S. Risse, R. Eberhardt, A. Tünnermann, Freeform Manufacturing of a Microoptical Lens Array on a Steep Curved Substrate by Use of a Voice Coil Fast Tool Servo, Optics Express, 19 (24) (2011), pp. 23938–23951

[7] E. Brinksmeier, et al., Submicron Functional Surfaces Generated by Diamond Machining, CIRP Annals – Manufacturing Technology, 59 (1) (2010), pp. 535–538

[8] B. Denkena, J. Kästner, B. Wang, Advanced Microstructures and Its Production Through Cutting and Grinding, CIRP Annals – Manufacturing Technology, 59 (1) (2010), pp. 67–72

[9] P. Guo, K.F. Ehmann, An Analysis of the Surface Generation Mechanics of the Elliptical Vibration Texturing Process, International Journal of Machine Tools and Manufacture, 64 (2013), pp. 85–95

[10] P. Guo, Y. Lu, K.F. Ehmann, J. Cao, Generation of Hierarchical Micro-structures for Anisotropic Wetting by Elliptical Vibration Cutting, CIRP Annals – Manufacturing Technology, 63 (1) (2014), pp. 553–556

[11] S. Xu, K. Shimada, M. Mizutani, T. Kuriyagawa, Fabrication of Hybrid Micro/Nano-textured Surfaces Using Rotary Ultrasonic Machining With One-Point Diamond Tool, International Journal of Machine Tools and Manufacture, 86 (2014), pp. 12–17

[12] R.-S. Lin, Y. Koren, Efficient Tool-Path Planning for Machining Free-Form Surfaces, Journal of Manufacturing Science and Engineering, 118 (1) (1996), pp. 20–28

[13] W. Zeng, X. Jiang, P.J. Scott, Fast Algorithm of the Robust Gaussian Regression Filter for Areal Surface Analysis, Measurement Science and Technology, 21 (5) (2010), pp. 1–9 055108

[14] P.J. Besl, N.D. McKay, Method for Registration of 3-D Shapes, Proceedings of SPIE 1611, Sensor Fusion IV: Control Paradigms and Data Structures (1992), pp. 586–606

[15] A. Hosokawa, T. Ueda, R. Onishi, R. Tanaka, T. Furumoto, Turning of Difficult-to-Machine Materials With Actively Driven Rotary Tool, CIRP Annals – Manufacturing Technology, 59 (1) (2010), pp. 89–92

[16] Y. Song, K. Nezu, C. Park, T. Moriwaki, Tool Wear Control in Single-Crystal Diamond Cutting of Steel by Using the Ultra-Intermittent Cutting Method, International Journal of Machine Tools and Manufacture, 49 (2009), pp. 339–343